Refined flicker photometry technique to measure ocular lens density

Petteri Teikari,[1,2,†,*] Raymond P. Najjar,[1,2,†] Kenneth Knoblauch,[1,2] Dominique Dumortier,[3] Pierre-Loïc Cornut,[4] Philippe Denis,[5] Howard M. Cooper,[1,2,6] and Claude Gronfier[1,2,7]

[1]*Stem Cell and Brain Research Institute, INSERM U846, 18 avenue Doyen Lepine, 69500 Bron, France*
[2]*Université Claude Bernard Lyon I, 69622 Villeurbanne Cedex, Lyon, France*
[3]*Housing Sciences, École Nationale des Travaux Publics de l'état, Rue Maurice Audin, 69518 Vaulx-en-Velin, France*
[4]*Department of Ophthalmology, CHU de Lyon Hôpital Edouard Herriot, 5 Place d'Arsonval, 69003 Lyon, France*
[5]*Department of Ophthalmology, Hôpital de la Croix-Rousse, 103 Grande Rue de la Croix-Rousse, 69317 Lyon, France*
[6]*e-mail: howard.cooper@inserm.fr*
[7]*e-mail: claude.gronfier@inserm.fr*
**Corresponding author: petteri.teikari@gmail.com*

Received September 21, 2012; revised September 21, 2012; accepted September 27, 2012;
posted September 28, 2012 (Doc. ID 167989); published October 24, 2012

Many physiological and pathological conditions are associated with a change in the crystalline lens transmittance. Estimates of lens opacification, however, generally rely on subjective rather than objective measures in clinical practice. The goal of our study was to develop an improved psychophysical heterochromatic flicker photometry technique combined with existing mathematical models to evaluate the spectral transmittance of the human ocular media noninvasively. Our results show that it is possible to accurately estimate ocular media density *in vivo* in humans. Potential applications of our approach include basic research and clinical settings on visual and non-image-forming visual systems.

OCIS codes: 170.4460, 330.4300, 330.4460, 330.5370, 330.5510, 330.7323.

1. INTRODUCTION

Many cellular and physiological processes in the eye follow a gradual decline during healthy aging. Although these processes are distinct from alterations resulting from ocular diseases in the aged, the resulting changes in vision may be similar, albeit smaller. Lens yellowing is one of these phenomena and gradually leads to cataracts [1], the most documented cause of blindness in developed countries. The relationship between healthy aging and ocular lens density has been studied by several groups [2–6]. These studies show a reduced transmission (increased density) of the crystalline lens, especially for short wavelength light. This decrease is even more pronounced in individuals with cataracts [4]. Psychophysical methods are easy to implement in both clinical and experimental settings. Recently Dillon *et al.* [7] and Broendsted *et al.* [8] demonstrated a significant correlation between a donor lens *ex vivo* technique and a noninvasive *in vivo* technique for assessing the human crystalline ocular media density.

In our study, we evaluated an improved inexpensive scotopic heterochromatic flicker photometry (HFP) technique that we designed and implemented to assess age-related changes in ocular media density. Spectral attenuation of the ocular media was approximated by fitting the obtained absorbance difference with the age-dependent human ocular media model of van de Kraats and van Norren [9]. The full spectral attenuation template allowed us to estimate photoreceptor-specific attenuation for a given subject. The HFP was compared to a previously described psychophysical technique of absolute threshold detection in the same subjects [2].

2. MATERIALS AND METHODS

Ocular media density in volunteer subjects was assessed using an improved light emitting diode (LED) driven HFP system developed at our institute (INSERM U846, Bron, France)

A. Principle of Ocular Media Transmission Measurement

Except for the crystalline lens and the macular pigment, the transmittance of the ocular media has been shown to be wavelength neutral and to show very little change in spectral transmittance with age [9]. Since the macular pigment has an effect mainly on the cones in the macula, a psychophysical procedure testing peripheral vision provides a good estimate of the ocular media density, without involvement of absorption by the macular pigment [4], and in an area of the retina that is rich in rods. The action spectrum of rhodopsin is genetically determined, stable with age, and well known [10]. When measuring aphakic individuals [11], the scotopic spectral sensitivity curve is highly similar to the relative absorption curve based on the extinction spectrum of rhodopsin [12]. Therefore, based on a nomogram [13] for rhodopsin sensitivity ($\lambda_{max} = 495$ nm; data from [14] refitted with [13], β-band included, and axial density d_{Rh} of 0.40 OD [15]), pairs of wavelengths with equal absolute threshold were chosen ($L1$ and $L2$). Without any filtering by the ocular lens *in vivo*, the scotopic thresholds for $L1$ and $L2$ are obtained at the same irradiance ($I1 = I2$). A different threshold is obtained ($I1 \neq I2$) when a spectral filtering of the light spectrum occurs due to the yellowing of the crystalline lens.

B. Subjects

Fifteen healthy adults participated in this study (seven males and eight females). Subjects were screened for medical health including medical history, physical exam, and ophthalmological exam. Subjects had normal color vision, visual field, and intraocular pressure, and did not have signs of ocular diseases. Subjects were grouped by age: five young (26.7 ± 4.5 years old), five middle aged (47.6 ± 4.0 years old), and five elderly (65.6 ± 4.7 years old).

The protocol was approved by the National Ethical Committee and all subjects gave written informed consent. Procedures were in compliance with the institutional guidelines and the Declaration of Helsinki. All experiments were performed between 9:00 and 19:00 and were conducted between January and July 2011.

C. Apparatus

The apparatus consisted of a test screen against a black background in front of a chin rest and a two-way joystick with a manual validation button (Fig. 1). The system was placed in a totally light-obscured black-painted room. A 3° wide annulus was implemented using LEDs that projected on a diffuser placed in front of the subject at a 15° to 18° eccentricity from visual (foveal) fixation. Foveal fixation to maintain gaze stability was provided by a dim red LED light (centered ≈10′ red fixation light, $\lambda_{peak} = 650$ nm, luminance of 7 to 10 cd/m^{-2}). The two LEDs used to produce the annular light stimulus had wavelength peaks at 405 nm (LedEngin, Inc., UV LED, LZ1-10UA00, 700 mA) and 530 nm (Philips Lumileds Luxeon III LED, LXHL-LM3C, 1000 mA). The LEDs were attached to heat sinks (Aavid Thermalloy, part No. 601403b06000) with a thermal adhesive (Aavid Thermalloy, Ther-O-Bond 1500) to ensure sufficient heat dissipation from the LEDs.

Light emitted by these LEDs was collimated (Ledil LE1-RS Lens, ±4° angle for 405 nm LED, and L2 3° Spot for the 530 nm LED) and filtered respectively by a 410 nm monochromatic filter (BFI Optilas IF 410 ± 0.4 nm, FWHM $= 3 \pm 0.4$ nm) and a 560 nm monochromatic filter (BFI Optilas IF 560 ± 0.4 nm, FWHM 3 ± 0.4 nm). The resulting chromaticity (CIE xy) for 410 nm light was $x = 0.18$, $y = 0.03$, and for the 560 nm light was $x = 0.41$, $y = 0.58$.

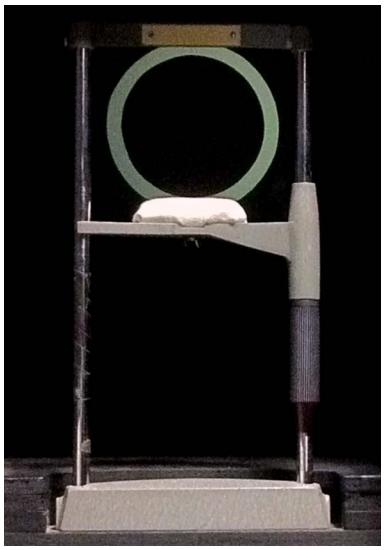

Fig. 1. (Color online) Physical lens density setup. The view of the annulus as seen by the subject. The subject positions himself to the chinrest and sees the annulus flickering in scotopic conditions.

Light intensity was attenuated to scotopic levels (10^{-2} to 10^{-6} cd/m^{-2}) by neutral density (ND) filters ranging from ND2.5 to ND5.0 (Omega Optical). ND filters used were dependent on individual scotopic thresholds. In practice, ND4.0 and ND4.5 were used for the 410 nm light and for the 560 nm light, respectively, for the young and middle-aged subjects, and ND3.0 and ND3.5 were used for the 560 nm light and for the 410 nm light, respectively, for the elderly subjects. The dynamic range of ≈2 log units of the light intensity was sufficient to take into account the individual variability among the age groups.

LEDs were driven by constant current LED drivers (XP Power LDU0830S350, 350 mA) and the intensity was controlled using a pulsewidth modulation (PWM) signal at a frequency of 400 Hz controlled by a data acquisition card (DAQ, National Instruments USB-6210). The software front-end was developed by the authors using LabVIEW development environment. The output current (350 mA) of the LED drivers was chosen to be lower than the nominal current of the LEDs to avoid reduction of light output and shift in the spectral peak emission with heating of the LEDs even with the heatsinks [16].

Light intensity was directly controlled by the subject, using the joystick. In order to increase or decrease light intensity, the subject pushed the joystick lever up or down. The joystick also had a validation button to acquire the subject's responses. Irradiance levels were monitored using a radiometer (International Light IL 1700) and a luminancemeter (Minolta LS-110). The spectral emission characteristics of the system were measured using a spectrophotometer (Ocean Optics USB4000). Data were analyzed using a custom-written MATLAB program (MathWorks).

The homogeneity of the light distribution in the visual field was quantified using the Photolux system [17]. The system consists of a Nikon 5000 digital camera with a fisheye lens and Photolux software developed in École Nationale des Travaux Publics de l'État (ENTPE) in Lyon, France. The observed homogeneity of the annulus was very good due to the use of multiple diffusing sheets (Fig. 2)

D. Methods

After instructions and protocol description, each participant was maintained in darkness for 45 min to ensure full dark adaptation (DA). This duration of DA allows 99.9% of the rhodopsin photopigment to be regenerated and responsive to light [18]. After the DA period, the participant underwent a training phase to learn how to operate the experimental setup.

The subject was instructed to adjust the intensity of a flickering annular light stimulus using a one-axis (up/+ or down/−) joystick, and to confirm his/her scotopic threshold intensity by pressing a button upon light detection. The annulus was displayed in the participant's peripheral visual field in a free/Newtonian view (3° wide, 15°–18° visual eccentricity). Results from free-view paradigms have been shown to correlate with results obtained with Maxwellian view [6], allowing simplification of an optical setup developed for macular pigment measurement [19]. Subjects gaze fixation was aided by the small dim red fixation LED light. Zagers and van Norren [20] suggested that the variability in their intrasession macular

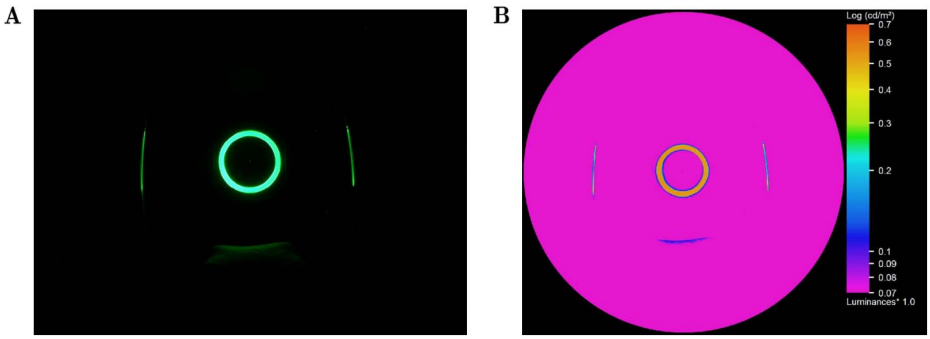

Fig. 2. (Color online) (A) Photo of the annulus with a long exposure time resulting in the color being a mixture of the 410 and 560 nm. The vertical reflections on the sides come from the chin rest metal frame, and one in the lower part of the annulus from the chin rest. (B) Corresponding luminance map with Photolux system [17]. The observed high homogeneity of the annulus is due to the use of multiple diffusing sheets.

pigment density resulted from fixation errors, with the less experienced subjects showing greater variability. Some of our subjects reported difficulties in fixating, and were instructed to briefly close their eyes for a few seconds, or blink repeatedly. An additional reason for allowing eye closure and blinking was to minimize the so-called Troxler's effect, a fading of the peripherally viewed stimulus that sometimes renders the extrafoveal flicker match difficult. All measures during the training period were conducted with the participant's nonpreferred eye, the preferred eye being occluded with an eye patch. On average, total measurement time including DA and instructions was about 90 min.

1. Absolute Scotopic Threshold Detection

Based on the principle described above, the absolute threshold technique provides an estimate of the ocular media density by directly comparing absolute scotopic thresholds to the rhodopsin absorption curve [2]. Such a comparison yields *in vivo* spectral density curves that generally agree with *ex vivo* curves suggesting the validity of this technique [11]. As stated by Wooten *et al.* [6], this technique is considered to be valid, as the response is rod-driven and relies on a univariant template, and provides *in vivo* spectral density curves that are usually in agreement with *ex vivo* curves.

While fixating a centered red dot with the preferred eye, the subject controls the annulus light intensity until the flickering annulus is detected in the peripheral visual field. The flicker frequency was chosen to be 2 Hz (500 ms of light, 500 ms of dark) based on a pilot study conducted in our laboratory and published temporal summation characteristics for scotopic vision [21]. The procedure was repeated five times with 410 nm light and five times with 560 nm light (Fig. 3). Under scotopic conditions both lights were perceived as gray (uncolored). Each trial yielded an estimate of the difference of quantal light intensities expressed as $\Delta I = I_{ph,410\ \mathrm{nm}} - I_{ph,560\ \mathrm{nm}}$ (both $I_{ph,410\ \mathrm{nm}}$ and $I_{ph,560\ \mathrm{nm}}$ being in log units), which was used for calculation of the ocular media density index (see Section 2). The possible diurnal variation of absolute threshold [22] has no influence on our results, as the variation has a symmetric effect for both test lights as the underlying spectral sensitivity is univariant.

2. Critical Fusion Frequency Detection

The aim of this step was to detect the subject's flicker sensitivity, also known as the critical fusion frequency (CFF [23]), in scotopic conditions optimizing the flicker frequency for subsequent tasks (see Section 2). The CFF is defined as the frequency for which intermittent light stimuli appears steady for the observer [24]. The initial goal of the CFF measurement was to use the obtained CFF for determination of an optimized individual flicker frequency as done when assessing macular pigment density with the heterochromatic flicker photometric (HFP) technique [25,26].

The CFF thresholds were obtained with the same optical design as in the above described absolute threshold method. Only the 560 nm reference light was used in this condition with a square-wave modulation at the maximal modulation depth (light was on half of the cycle period, and off the other half of the cycle). The intensity of the 560 nm light was set at one log unit above the individual absolute threshold, and its flicker frequency (range of 0.2–60 Hz) was controlled by the subject using the joystick (method of adjustment).

Subjects were instructed two approaches (Fig. 3): (1) start the flickering of the annulus by decreasing its flicker frequency

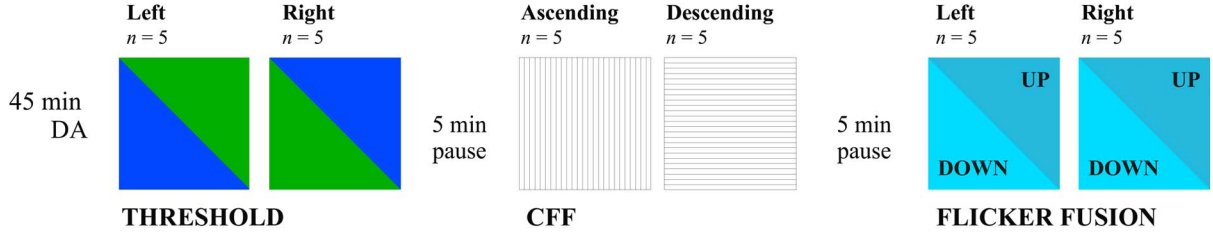

Fig. 3. (Color online) Ocular media density measurement protocol. After 45 min of DA, subjects performed a threshold detection training phase with the nonpreferred eye ('nondominating', left for majority of the subjects) and were instructed to increase the light intensity of the 560 nm light until the detection of the annulus was flickering. Training was followed by a threshold detection procedure for 560 and 410 nm lights with the preferred eye. In a second step subject had to detect their CFF by increasing (ascending) or decreasing (descending) annulus flickering frequency. In the last step of the protocol (flicker fusion) the subject had to abolish or minimize their perception of flickering by adjusting intensity of a 410 nm light either by increasing it (UP) or decreasing it (DOWN). Flicker fusion was made using both eyes, starting with the nonpreferred eye.

(descending condition), and (2) stop the flickering of the annulus by increasing its flicker frequency (ascending condition). Both the ascending and the descending conditions were repeated five times. The CFF threshold was considered to be the frequency for which the subject detected the annulus flickering while decreasing its frequency (mean of all trials). The latter option of decreasing the frequency was shown to be less affected by flicker adaptation, lowering the CFF of the subject with increased exposure to flickering light [27]. CFF has been shown to have high test–retest reliability [28]; thus the obtained CFF can be considered a reliable estimate for our purposes.

3. Heterochromatic Flicker Photometry

Ocular media density was assessed using the HFP technique [29], in which the subjects were instructed to minimize or eliminate the perception of flicker by adjusting the light intensity of the test light (410 nm light) while the reference (560 nm light) was kept constant. The HFP technique has been validated for macular pigment (MP) measuring the entire spectral absorption curve, which closely matched the *ex vivo* measurement of the MP absorption spectrum [30].

The 410 nm (test light) and the 560 nm (reference light) lights were square wave-modulated in counter-phase with a frequency of 2 Hz (500 ms of test, 500 ms of reference, as used by [6]), which was found to provide reliable results from all subjects. Barbur *et al.* [31] observed that subjects with a low CFF have a wide flicker nulling range, while subjects with high CFF may not be able to null the perception of flicker completely, particularly when the fixation instability is large. The nulling range is defined as the difference between flicker null intensity while approaching the flicker null zone with increasing intensity and with decreasing intensity.

The 560 nm light was set one log unit above each participant's threshold (determined previously), and the subject had to adjust the light intensity of the 410 nm light in order to stop the perceived flickering of the annulus. Since both lights are still seen as gray (uncolored) under these scotopic conditions complete fusion of the two flickering stimuli can only be achieved when both lights are perceived to be of equal intensity. At this point the difference between the intensities of two wavelengths provides an index of the ocular media density. The subject was instructed to perform the adjustment by first increasing the 410 nm light intensity, and then decreasing the light intensity. The fusion point was calculated as the mean of these two measures (end points of nulling range) as done previously by Barbur *et al.* [31]. Both eyes were tested individually and five trials were obtained for each condition and each eye. The ocular media density was calculated as with the absolute scotopic threshold detection (see Section 2).

Criterion measures obtained with the method of adjustment are subject to observer biases, which might be controlled using, for example, signal detection measures. Such approaches, however, are much more time consuming. Given that performance is mediated by the quantum catch rate for a single photopigment, we assume the results to obey univariance and we expect that any biases would be independent of wavelength. The lens density estimates, however, are based on the ratio of values at two different wavelengths. Thus, multiplicative (but not necessarily additive) biases would tend to cancel. In addition, for the flicker measures, the use of a bracketing procedure and the choice of temporal frequency to minimize the extent of the flicker-free null zone would also tend to minimize bias.

4. Ocular Media Density Index Calculation

The ocular media density index was calculated from the obtained detection difference of the scotopic threshold condition (Section 2) and the flicker null of the HFP condition (Section 2) $\Delta I = I_{ph,410\ \mathrm{nm}} - I_{ph,560\ \mathrm{nm}}$ based on the formulation of van Norren and Vos [2]. The average ocular media density difference D_{stdDiff} between the used spectral power distributions of the experimental lights (photon densities $L_1(\lambda)$ for 410 nm and $L_2(\lambda)$ for 560 nm in linear scale) was calculated from the standard observer ocular media density $D_{\mathrm{stdObs}}(\lambda)$ from the human ocular media model of van de Kraats and van Norren [9] by setting the parameter "age" to 25 years [see Eq. (9) later for details]:

$$D_{\mathrm{stdDiff}} = \log_{10} \int_{380}^{780} \left(\frac{L_1(\lambda) \times 10^{D_{\mathrm{stdObs}}(\lambda)} \mathrm{d}\lambda}{L_2(\lambda) \times 10^{D_{\mathrm{stdObs}}(\lambda)} \mathrm{d}\lambda} \right). \tag{1}$$

Now the obtained D_{stdDiff} is the same as the "scaling factor" used in [2], and for our choice of experimental lights the D_{stdDiff} was ≈0.775 log units. This approach of integrating the "effective ocular media density" over the full light spectrum (from 380 to 780 nm) avoids the cumbersome use of tabulated values of van Norren and Vos [2] that are only valid for monochromatic lights, in practice being of a relevance with unfiltered LEDs as pointed out by Wooten *et al.* [6].

The ocular media density index $D_{\mathrm{ocularMedia}}$ for each subject is calculated by subtracting the ΔI from the obtained D_{stdDiff}:

$$D_{\mathrm{ocularMedia}} = D_{\mathrm{stdDiff}} - \Delta I. \tag{2}$$

The ocular media density index $D_{\mathrm{ocularMedia}}$ now represents the difference in ocular media density between the model "standard observer" and the subject tested, and thus can be negative if the subject has a very low ocular media density or due to calibration offsets in the system. The $D_{\mathrm{ocularMedia}}$ is the ideal ocular media density assuming that our two short $L_1(\lambda)$ and long $L_2(\lambda)$ wavelength test lights equally stimulated rhodopsin and the spectral transmittance of the measurement system was spectrally neutral. However, this was not the case and the following corrections have to be made for the $D_{\mathrm{ocularMedia}}$.

First, our method is sensitive to the correct parameters chosen for the rhodopsin peak wavelength λ_{max}, the peak density d_{Rh}, and the nomogram model for rhodopsin $S(\lambda)$, as pointed out by van de Kraats and van Norren [9] in regard to the previously published method from the same authors [2]. In practice the experimental lights do not have to stimulate equally rhodopsin if the stimulation difference ΔR between the used experimental lights is exactly known and expressed as follows:

$$\Delta R = \log_{10} \int_{380}^{780} \left(\frac{L_1(\lambda) \times S(\lambda) \mathrm{d}\lambda}{L_2(\lambda) \times S(\lambda) \mathrm{d}\lambda} \right). \tag{3}$$

In the paper by van Norren and Vos [2], peak wavelength λ_{max} was chosen to be 493 nm [32], and the peak density d_{Rh} of 0.20 [33] while using the Dartnall template [34]. We chose slightly different values based on recent literature with a peak wavelength λ_{max} estimate of 495 nm by refitting the points given by Kraft *et al.* [14] with the nomogram provided by

Govardovskii *et al.* [13]. The self-screening [35] correction was done with an estimate of 0.40 for peak density d_{Rh} for rhodopsin in dark-adapted human rods [15] as follows:

$$S(\lambda)_{ss} = \log_{10}\left\{\frac{1 - [S(\lambda) \cdot (1 - 10^{-d_{Rh}})]}{-d_{Rh}}\right\}, \tag{4}$$

where $S(\lambda)_{ss}$ is the spectral sensitivity for rhodopsin, corrected for the self-screening effect. The length of the human rod outer segment is 25 μm [36]; thus the correction for spectral absorbance change as a function of outer segment length was found to be insignificant with human rhodopsin [37]. With our parameter values the 410 nm light stimulated 0.08 log units more of the rhodopsin than the used 560 nm light, whereas with the parameter values of van Norren and Vos [2], our 410 nm light would have stimulated 0.19 log units more of the rhodopsin than the 560 nm light.

The self-screening effect of rhodopsin peak density d_{rh} had a negligible effect on rhodopsin stimulation; decreasing d_{rh} from 0.40 to 0.20 caused a simulated increase of 0.004 log units in rhodopsin stimulation at $\lambda_{max} \approx 495$ nm. The results of these calculations are shown in Fig. 4. The insensitivity of our method to pigment density d_{rh} is beneficial as there is a possibility that the rhodopsin pigment density changes with age [38], while some reports have found rhodopsin photopigment density to vary little with age [39].

Additionally, the apparatus with its diffusing sheets differentially filtered short-wavelength light especially due to Rayleigh scattering causing blue light to scatter more and to be attenuated significantly in the optical path of the apparatus [40]. The apparatus was measured to attenuate our 410 nm test light 0.60 log units more than the 560 nm test light.

5. Estimation of Spectral Attenuation from Ocular Media Density Index

The human ocular media model $D_{\text{media}}(\lambda)$ defines the human ocular media in general form as a sum of five spectral components and a spectrally neutral offset:

$$\begin{aligned} D_{\text{media}}(\lambda) = {} & d_{\text{RL}}(\text{age}) \times M_{\text{RL}}(\lambda) + M_{\text{TP}}(\lambda) + d_{\text{LY}}(\text{age}) \\ & \times M_{\text{LY}}(\lambda) + d_{\text{LOUV}}(\text{age}) \times M_{\text{LOUV}}(\lambda) + d_{\text{LO}}(\text{age}) \\ & \times M_{\text{LO}}(\lambda) + d_{\text{neutral}}, \end{aligned} \tag{5}$$

where M_i are the templates (M for media) describing the spectral shape of each component and d_i are age-dependent scalar weights, i.e., the density coefficients. The subscripts RL, TP, LY, LOUV, and LO are Rayleigh loss, tryptophan, lens young, lens old UV, and lens old, respectively.

The templates M_{TP} and M_{RL} represent the light losses in the ocular media as a whole; the former is based on tryptophan absorption occurring heavily below 310 nm [41] and extending to short wavelength light, and the latter for Rayleigh scatter

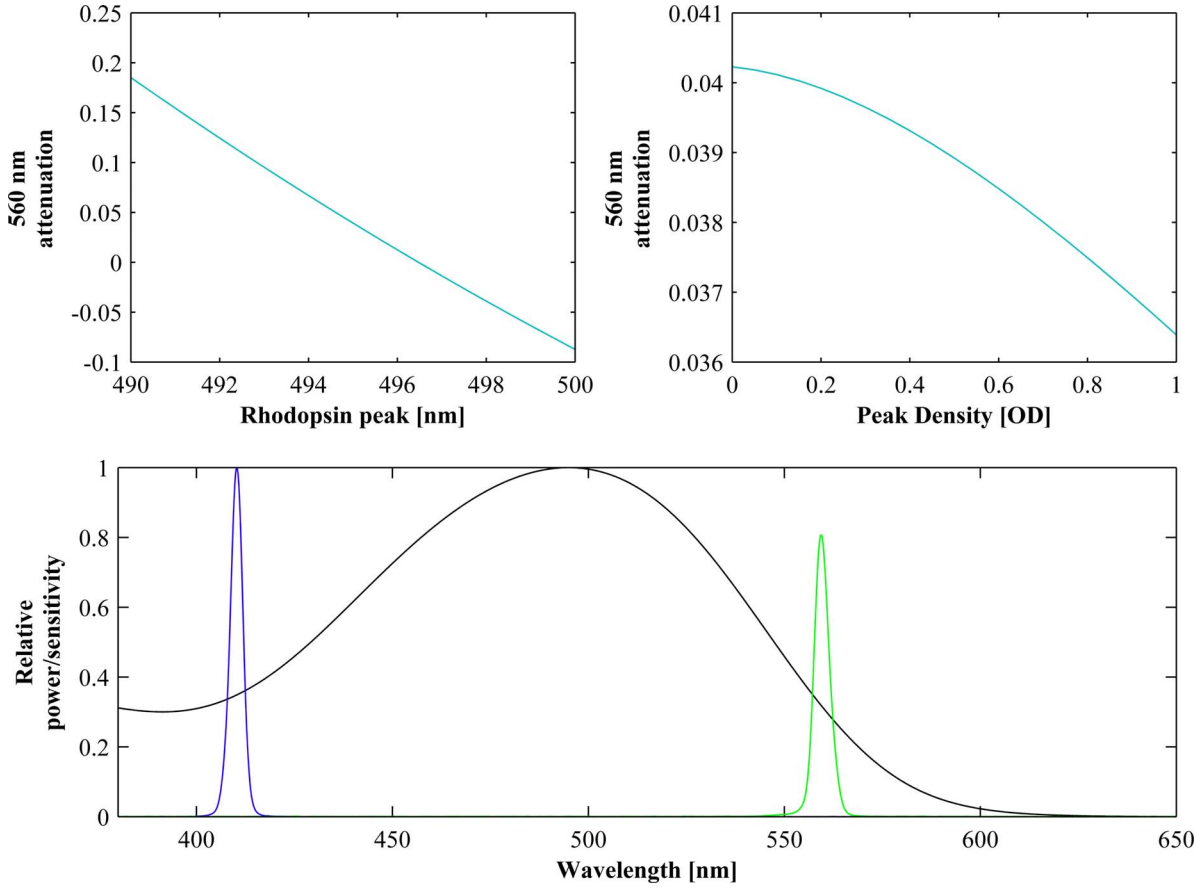

Fig. 4. (Color online) Sensitivity of the method for rhodopsin parameters. Separate analysis for rhodopsin peak sensitivity λ_{max} (left, above) and rhodopsin axial pigment density d_{rh} (right, above). Values used by us are $\lambda_{max} = 495$ nm and $d_{rh} = 0.40$. The nomogram of Govardovskii *et al.* [13] includes the β-band; thus the short-wavelength lobe is elevated. The lights are normalized to have the same total photon density; thus the green 560 nm has a lower peak value.

arising from light interaction with submicroscopic density fluctuations in the ocular media including the aqueous and vitreous humors [42], and cornea [43,44]. Without the Rayleigh scatter, the humors and the cornea can be considered to be spectrally neutral absorbers as they consist mainly of water [45]. The aqueous component in the eye starts to absorb beyond 700 nm and the transmittance can be modeled then using the tabulated water absorption up to 2500 nm [46].

The three lens templates (LY, LOUV, and LO) are based on the absorbance characteristics of kynurenine derivatives [47] in the human eye, dominating absorbers being the the 3-hydroxy-kynurenine glucoside (3HKG) with contributions from kynurenine and 3-hydroxy-kynurenine. With aging, the lens proteins undergo changes in structure or in binding of kynurenine products [48]; for example, the total amount of 3HKG is reduced to about 30% at the age of 50 compared to the young lens [47]. The three lens templates and the tryptophan template can be described with a single Gaussian:

$$M_{i,\mathrm{gaussian}} = \mathrm{norm} \times \exp(-\{[w \times (\lambda - \lambda_{\mathrm{peak}})]^2\}), \quad (6)$$

where norm is the normalization factor for the template to normalize the template to unity at 300 nm, w is the width factor (in nm^{-1}) describing the "narrowness" of the spectral template analogous to the definition of half-bandwidth in Gaussian light sources, and the λ is the wavelength vector and the λ_{peak} is a scalar wavelength describing the maximum absorption of the spectral template. The Rayleigh scatter component M_{RL} is described as a monotonically decreasing function with wavelength, typical for Rayleigh scatter:

$$M_{\mathrm{RL}}(\lambda) = (400/\lambda)^4. \quad (7)$$

The age relationship for d_i was found by the authors [9] best described by a quadratic age relationship rather than by a linear one:

$$d_i = d_{i,0} + \alpha_i \times \mathrm{age}^2 \quad (8)$$

with $d_{i,0}$ the density at age 0 (the intercept), α_i the aging in years^{-2} (quadratic slope), and age in years.

The human ocular media model $D_{\mathrm{media}}(\lambda)$ can be expressed in its final form [Eq. (9)] with all the numerical values derived by van de Kraats and van Norren [9], combining the Gaussian expression [Eq. (6); for TP, LY, LOUV, and LO] and Rayleigh scatter [Eq. (7)] with the aging trend [Eq. (8); excluding M_{TP}, which was not found to depend on age] resulting in the following:

$$\begin{aligned} D_{\mathrm{media}}(\lambda) = {} & (0.446 + 0.000031 \times \mathrm{age}^2) \times (400/\lambda)^4 \\ & + 14.19 \times 10.68 \times \exp(-\{[0.057 \times (\lambda - 273)]^2\}) \\ & + (0.998 - 0.000063 \times \mathrm{age}^2) \times 2.13 \\ & \times \exp(-\{[0.029 \times (\lambda - 370)]^2\}) \\ & + (0.059 - 0.000186 \times \mathrm{age}^2) \times 11.95 \\ & \times \exp(-\{[0.021 \times (\lambda - 325)]^2\}) \\ & + (0.016 - 0.000132 \times \mathrm{age}^2) \times 1.43 \\ & \times \exp(-\{[0.008 \times (\lambda - 325)]^2\}) + 0.111. \end{aligned} \quad (9)$$

Strictly speaking, the individual spectral templates could vary independently in relation to each other, and with our two-wavelength approach it may not possible to capture the individual spectral variations.

The ocular media density index was calculated by fitting the ocular media model of van de Kraats and van Norren [9] to the measured density difference between the measured wavelengths (410 and 560 nm). The difference was converted to two data points by arbitrarily fixing the 560 nm to arbitrary density of zero and the data point 410 nm below the measured lens density, with only the age as a free parameter in the numerical optimization (Matlab function fmincon, from Optimization Toolbox) in the model [Eq. (9)] resulting in a "virtual age" estimate for each subject. This virtual age is conceptually similar to the virtual age used by van Norren and van de Kraats [49] to estimate the spectral behavior of intraocular lenses in regard to their photoreception and the photoprotection characteristics. Virtual age of the lens allowed us to estimate the full spectral attenuation profile of the ocular media.

3. RESULTS

A. Fusion versus Threshold Method

The ocular media density index, when plotted as a function of squared age (age^2 as done in [9]), shows an increasing trend with age in both the HFP condition (Fig. 5A) and the absolute scotopic threshold condition (Fig. 5B). However, the HFP measure exhibits a stronger correlation with age ($R^2 \approx 0.79$ for the HFP, $R^2 \approx 0.42$ for the scotopic thresholds. The scotopic threshold condition underestimates the effect of aging to ocular media density ($a_i = 0.000107$) compared to the results obtained in HFP condition ($a_i = 0.000155$). The results are normalized with the absorbance difference D_{stdDiff} [see Eq. (1)] of our test lights (410 and 560 nm) obtained from the ocular media model of [9] setting the age to 25 years old, corresponding to the use of "scaling factor" [2].

Results in 15 subjects (five young, five middle aged, and five old) show a significant effect of age group on ocular media density index (ANOVA, $F(2, 12) = 26.5$, $p < 0.0001$). Post hoc analysis showed a significant difference between the young and the elderly groups (Student Newman-Keuls, $p < 0.001$), and between the middle-aged and the elderly groups (Student Newman-Keuls, $p < 0.001$). Although there was an increase in ocular media density between the young and the middle-aged groups, this difference was not statistically significant ($p < 0.1$). Interindividual variability increased with age (group mean ± SD: young (0.009 ± 0.067), middle-aged (0.167 ± 0.049), elderly (0.619 ± 0.22) group.

B. Spectral Transmittance Profiles

Employing the obtained ocular media density values with the ocular media model by van de Kraats and van Norren [9] (calculations outlined in Section 2) yielded diminished transmittance over the entire visible spectrum in the old-age group compared to the young and the middle-aged groups (shown in Fig. 6). The filtering of the ocular media is particularly pronounced in the short wavelength range (<500 nm)

C. CFF

No age-dependent effect was found for CFF threshold. The results are in accordance with the three-phase age dependence of temporal contrast sensitivity (TCS, i.e., flicker sensitivity), TCS increasing up to an age of ≈16 years, then

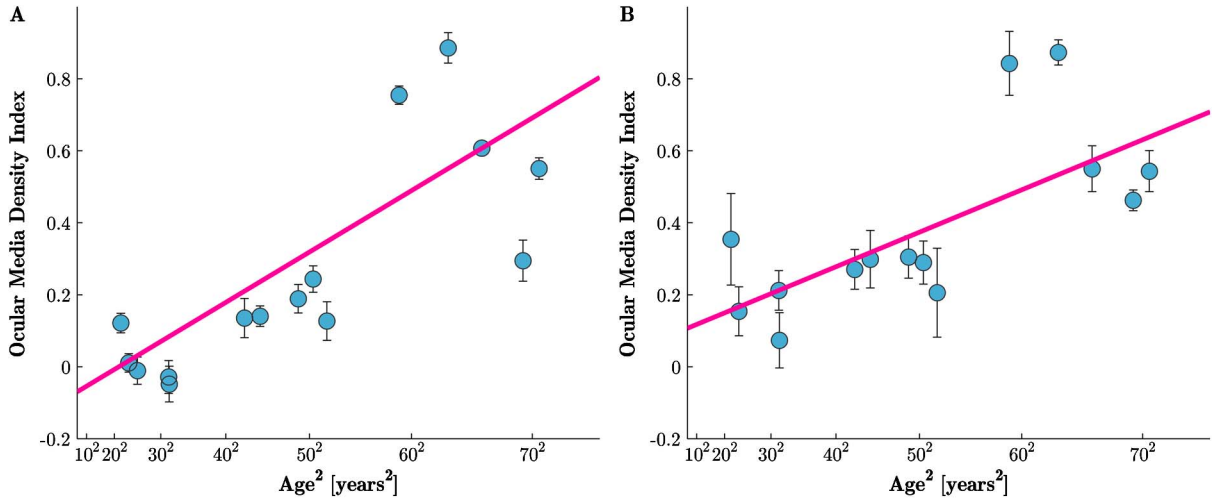

Fig. 5. (Color online) Ocular media density index as a function of age, (A) estimated using the HFP technique (age coefficient $a_i = 0.000155$ [Eq. (8)], $R^2 \approx 0.79$), and (B) using the absolute scotopic threshold condition (age coefficient $a_i = 0.000107$ [Eq. (8)], $R^2 \approx 0.42$). All values are given as mean ± SD.

remaining relatively constant until 60 years followed by a decline after 60 years [50,51].

We found no systematic association between nulling range and CFF. For one subject, the dynamic range of our light setup was insufficient for the descending HFP condition, so that this subject was unable to detect any flicker at the highest 410 nm light intensity and flicker frequency of 2 Hz, although with a flicker frequency of 5 Hz the detection was possible.

4. DISCUSSION

Our results confirm that short-wavelength light absorption by the ocular media increases with age [3,9,52]. The obtained difference of 0.61 between the D_{lens} of the young and the old age groups is in accordance with previous studies [53,54]. Similarly, the aging trend, a_i, (year^{-2}) of 0.000155 we obtained using the HFP technique is similar to those obtained by psychophysical methods [9], but higher than a_i obtained for donor lenses, as noted already by van de Kraats and van Norren [9]. The full spectrum approximation of transmittance depends on the quality of the ocular media model of van de Kraats and van Norren [9]. A recent study by Gimenez *et al.* [55] used objective reflectometric techniques to measure ocular media density, and showed a close correspondence with the prediction of the human ocular model of van de Kraats and van Norren [9], confirming its validity.

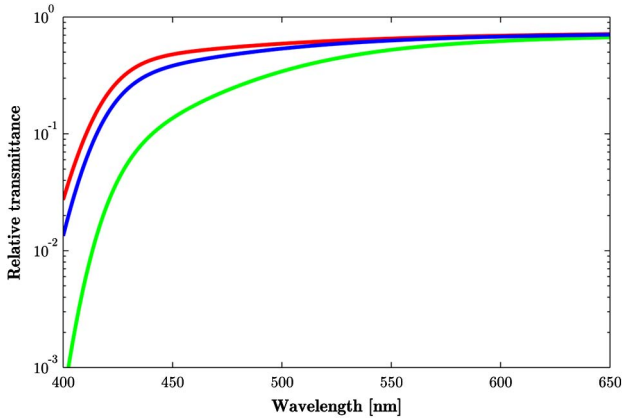

Fig. 6. (Color online) Relative spectral transmittance of the three age groups as derived using the virtual age with the model of [9]: young group (top, red curve), middle-aged group (middle, blue curve), and elderly group (bottom, green curve). Young, $\text{age}_{\text{virtual}} = 23.38(-7.6 \quad +5.0)$; middle, $\text{age}_{\text{virtual}} = 40.32(-3.8 \quad +3.6)$; elderly, $\text{age}_{\text{virtual}} = 88.81(-1.8 \quad +2.1)$.

The relatively high inter-individual variability in the ocular media density that we found in this study, especially in the old age group, confirms previous results [4]. This finding supports the notion that in many cases the use of average values of ocular media density for a given age are not indicative of an individual crystalline lens density. While mathematical models have been produced to predict the expected changes in the absorption characteristics of the aging lens [3,9,20], they cannot reflect the individual variability occurring with real observers, and they cannot accurately predict lens density from age for a given individual. This is in contrast with the typical preretinal absorbance corrections applied using a standardized ocular media density template (e.g., [56]), for example, in studies on perceptual [57] and non-image-forming (NIF) visual system [58].

Strictly speaking, the current psychophysical HFP method cannot distinguish the crystalline lens component from the other ocular absorbers, and the obtained result is an estimate of the whole eye absorption difference between the 410 and the 560 nm light. By choosing a peripheral retinal location of the light stimulus (3° wide annulus at retinal eccentricities between 15° to 18°), the contribution of the macular pigment was avoided [59]. Even considering the noted variability in the peak density of the macular pigment, the rate of spatial decrease of the macular pigment amongst individuals [60], and the possible spread of the macular pigment toward the periphery of retina with age [61], the chosen retinal eccentricity can be assumed to be free from macular pigment intrusion. The cornea and the aqueous and the vitreous humors were implicitly incorporated to the human ocular media model of van de Kraats and van Norren [9], and their contribution to the obtained ocular media density results cannot be distinguished. In previous reports, however, the optical density contribution of the cornea [43,62] and the humors [43] were found not be effected by aging, making their contribution to the obtained ocular media density estimate constant with age.

Additionally, marked differences in the aging factor [d_{RL}(age), Eq. (5)] of the scatter component [$M_{RL}(\lambda)$ in Eq. (7)] between psychophysical data and the donor lenses had been noticed by van de Kraats and van Norren [9]. This difference, if real, was attributed to either the existence of an additional scatter source at the retinal level and/or compensation for scatter in the donor lens measurements. This reported difference was already in contrast with the absence of aging of d_{RL}(age) with the reflection-based measurements most likely being caused by relative large detector angles used in those type of measurements [9]. Thus, one could argue that our psychophysical estimates can overestimate the age-related increase of ocular media density.

In a study of Van Loo and Enoch [63], a wavelength-dependent directionality was found for the human rods in a Maxwellian view setup. The extreme directionality difference at 3.5 mm displacement from the center of the pupil was found to be 0.17 log units between the used monochromatic 433 nm light and the broadband light with wavelengths below 433 nm being filtered out. The directionally difference was found to be negligible up to 1.5 mm displacement from the center, and combining this with our approach to use the free-view optical setup, the directionality for the used wavelengths can be assumed to be nonexistent.

The crystalline lens has been shown to fluoresce in response to light mainly at two spectral bands, the blue fluorescence and the green fluorescence [64]. Excitation of the lens at 413 nm causes a fluorescence emission with a peak at ≈480 nm [65]. Fluorescence may be assumed to add a uniform component to the retinal point spread function degrading visual performance by adding a "veiling glare" on top of the retinal image [66]. Weale [67] estimated the reciprocal ratio between the luminance of a patch of sky and the fluorescence it induces to be ≈0.002 for the normal lens of a 30-year-old human, increasing to 0.017 for a 60 year old, and to 0.121 for an 80 year old, the two latter ones starting to be visually noticeable. The intensity of fluorescence increases roughly linearly with age [64], and with fluorophores emerging that emit at even longer wavelengths [68,69]. The upper wavelength limit for the excitation is around 650 nm for older lenses [69]. The absorbance of fluorescence by the ocular media itself has been also used to quantify the lens absorption [8,70].

As the induced fluorescence outlasts the duration of the exciting stimulus (500 ms in our setup), it can be assumed that in our psychophysical paradigm there is an added "visual stimulus" both during the 410 nm light and decaying fluorescence during the 560 nm light. The exact "glare luminance" depends on the photon densities at a given time. Van den Berg [71] estimated quantal sensitivity of the blue fluorescence (induced, for example, by our 410 nm light) to be between 0.004 and 0.025 fluorescent quanta per exciting quantum. The putative visual impairment is qualitatively similar to the "flash blindness" phenomenon [72] as referred in Zuclich *et al.* [65]. Lens fluorescence causes a prolonged glare/visual impairment, for example, from the blue-enriched headlights of passing cars in nighttime driving conditions [73].

In theory, the transmural transmittance of the ocular wall and iris transmittance could have contributed to our results by attenuating the test light at 410 nm more than the 560 nm reference light; however, the attenuation values found in the literature were in order of 2 log units for white light, even for light-eyed subjects [74]. These estimated iris transmittance values combined with the dark-adapted pupil in our scotopic condition, leading to a smaller iris area, and the effect of iris transmittance in our ocular media density values can be assumed to be insignificant.

There has been some evidence of other sources of yellowing of the ocular media existing in the human eye. Geeraets *et al.* [75] found short-wavelength absorption in the human neurosensory retina (outside the macula), while at that time it was considered to be a postmortem artifact. The report of Snodderly *et al.* [76] suggest the existence of two additional yellow pigments with absorbance maxima at 410 and 435 nm, located in the outer nuclear layer or the inner segment layer of retinal tissue both inside and outside the anatomic fovea. Furthermore, Bowmaker *et al.* [77] reported another yellow ocular pigment, located in the inner segments of both rods and cones of old-world monkeys with a peak absorbance at 420 nm. Any or all of these yellow pigments could contribute to the filtering of the light before reaching the rods in our scotopic measurement conditions. Additionally, photoreversal of rhodopsin bleaching [78,79] and putative retina G protein-coupled receptor mediated rhodopsin regeneration [80,81] can influence our measures, but their significance to our measurements was estimated to be minor.

The HFP technique has been widely used to measure OD of the macular pigment. To our knowledge, only three studies have utilized HFP to measure ocular lens density [6,31,82] outside the macular pigment. Compared to these studies, we believe our approach is an improved technique to assess optical lens density for the following reasons: (1) Our proposed methodology to measure lens density is based on a simple and inexpensive LED-based apparatus and HFP procedure that can easily be implemented in other laboratories, as demonstrated recently also for measuring macular pigment density [83]. (2) Our HFP approach reduces interindividual and intraindividual variability. Compared to Wooten *et al.* [6], who obtained an SD of 0.22 log OD for his group of 30 subjects aged 24 ± 7 yrs, we obtained an SD of 0.06 log OD for the same age range ($n = 5$) in this study, and of 0.08 log OD in another study ($n = 19$, published elsewhere). (3) Compared to the classical threshold detection technique, our results show that the HFP technique significantly reduces intraindividual variability (average SD HFP = 0.039, average threshold SD = 0.077). The intra-individual trial variability is significantly reduced when using the HFP method (t-test, $p = 0.003$). (4) Our protocol makes use of a bracketing procedure to assess flicker fusion (nulling range). Such a procedure ought to minimize biases due to different stimulus detection approaches (which could occur, for example, in the elderly who are known to follow a more conservative psychophysical approach [84]. (5) The two wavelengths we selected in our HFP procedure (410 and 560 nm) are believed to yield the exact same scotopic sensitivity [2,4]. The most recent template for photopigments sensitivity [13], however, shows minor differences in sensitivities between 410 and 560 nm (Fig. 4). Therefore, we took into account this difference to correct the ocular density index, and we used the most recent template to approximate spectral lens transmittance from the ocular media density index [9].

In conclusion, our psychophysical method is able to provide a precise, yet relatively inexpensive estimate of the

ocular media density, which is a clear improvement compared to the approach of using standardized ocular media templates. Such estimates are of major relevance in studies regarding photoreception where estimation of retinal spectral irradiance is essential. We are currently optimizing our procedure by reducing the DA time with the intention to eliminate it entirely in order to make this technique more practical, both for the subject and for the experimenter in research and clinical settings.

For further improvement of the spectral resolution of the approximation of the ocular media transmittance, additional test wavelengths could be employed, for example, at the wavelength region of 480 nm corresponding to the peak spectral sensitivity of melanopsin [85] and for several NIF responses [86,87]. In that case two distinct heterochromatic flicker pairs (410 nm versus 560 nm, and 480 nm versus 560 nm) would need to be done for each subject. This would result in three points for the curve-fitting algorithm (Section 2), thus improving the accuracy of the full spectral attenuation estimate.

ACKNOWLEDGMENTS

Financial support: ANR-09-MNPS-040, the European Union (FP6-EUCLOCK) (http://www.euclock.org/), Retina France, Unadev, Rhône-Alpes Cible, Rhône-Alpes Cluster HVN, Federation des Aveugles et Handicapés Visuels de France, and Ministère de l'Enseignement Supérieur et de la Recherche Français.

†These authors contributed equally to this work.

REFERENCES

1. R. Michael and A. J. Bron, "The ageing lens and cataract: a model of normal and pathological ageing," Philos. Trans. R. Soc. B **366**, 1278–1292 (2011).
2. D. van Norren and J. J. Vos, "Spectral transmission of the human ocular media," Visual Res. **14**, 1237–1244 (1974).
3. J. Pokorny, V. C. Smith, and M. Lutze, "Aging of the human lens," Appl. Opt. **26**, 1437–1440 (1987).
4. P. Sample, F. Esterson, R. Weinreb, and R. Boynton, "The aging lens: in vivo assessment of light absorption in 84 human eyes," Invest. Ophthalmol. Vis. Sci. **29**, 1306–1311 (1988).
5. C. A. Johnson, D. L. Howard, D. Marshall, and H. Shu, "A noninvasive video-based method for measuring lens transmission properties of the human eye," Optom. Vis. Sci. **70**, 944–955 (1993).
6. B. R. Wooten, B. R. Hammond, and L. M. Renzi, "Using scotopic and photopic flicker to measure lens optical density," Ophthalmic Physiol. Opt. **27**, 321–328 (2007).
7. J. Dillon, L. Zheng, J. C. Merriam, and E. R. Gaillard, "Transmission of light to the aging human retina: possible implications for age related macular degeneration," Exp. Eye Res. **79**, 753–759 (2004).
8. A. E. Broendsted, M. Stormly Hansen, H. Lund-Andersen, B. Sander, and L. Kessel, "Human lens transmission of blue light: a comparison of autofluorescence-based and direct spectral transmission determination," Ophthalmol. Res. **46**, 118–124 (2011).
9. J. van de Kraats and D. van Norren, "Optical density of the aging human ocular media in the visible and the UV," J. Opt. Soc. Am. A **24**, 1842–1857 (2007).
10. H. J. Dartnall, J. K. Bowmaker, and J. D. Mollon, "Human visual pigments: microspectrophotometric results from the eyes of seven persons," Proc. R. Soc. Lond. Ser. B **220**, 115–130 (1983).
11. M. S. Griswold and W. S. Stark, "Scotopic spectral sensitivity of phakic and aphakic observers extending into the near ultraviolet," Vis. Res. **32**, 1739–1743 (1992).
12. G. Wald, "The photochemistry of vision," Doc. Ophthalmol. **3**, 94–137 (1949).
13. V. I. Govardovskii, N. Fyhrquist, T. Reuter, D. G. Kuzmin, and K. Donner, "In search of the visual pigment template," Vis. Neurosci. **17**, 509–528 (2000).
14. T. W. Kraft, D. M. Schneeweis, and J. L. Schnapf, "Visual transduction in human rod photoreceptors," J. Physiol. **464**, 747–765 (1993).
15. T. Lamb, "Photoreceptor spectral sensitivities: common shape in the long-wavelength region," Vis. Res. **35**, 3083–3091 (1995).
16. N. Pousset, B. Rougi, and A. Razet, "Impact of current supply on LED colour," Lighting Res. Technol. **42**, 371–383 (2010).
17. D. Dumortier, B. Coutelier, T. Faulcon, and F. Roy, "PHOTOLUX: a new luminance mapping system based on Nikon Coolpix digital cameras," in *Proceedings of Lux Europa* (Lux Europa, 2005), pp. 308–311.
18. O. A. R. Mahroo and T. D. Lamb, "Recovery of the human photopic electroretinogram after bleaching exposures: estimation of pigment regeneration kinetics," J. Physiol. **554**, 417–437 (2003).
19. O. Howells, F. Eperjesi, and H. Bartlett, "Measuring macular pigment optical density in vivo: a review of techniques," Graefes Arch. Clin. Exp. Ophthalmol. **249**, 315–347 (2011).
20. N. P. A. Zagers and D. van Norren, "Absorption of the eye lens and macular pigment derived from the reflectance of cone photoreceptors," J. Opt. Soc. Am. A **21**, 2257–2268 (2004).
21. S. Hecht, S. Shlaer, and M. H. Pirenne, "Energy, quanta and vision," J. Gen. Physiol. **25**, 819–840 (1942).
22. C. J. Bassi and M. K. Powers, "Daily fluctuations in the detectability of dim lights by humans," Physiol. Behav. **38**, 871–877 (1986).
23. J. D. Conner, "The temporal properties of rod vision," J. Physiol. **332**, 139–155 (1982).
24. H. E. Ives, "Critical frequency relations in scotopic vision," J. Opt. Soc. Am. **6**, 254–267 (1922).
25. B. R. Hammond and B. R. Wooten, "CFF thresholds: relation to macular pigment optical density," Ophthalmic Physiol. Opt. **25**, 315–319 (2005).
26. K. O'Brien, B. Smollon, B. Wooten, and B. Hammond, "Determining heterochromatic flicker photometry frequency for macular pigment optical densitometry by critical flicker fusion frequency," J. Vis. **11**, 55–55 (2011).
27. R. Nygaard and T. Frumkes, "Frequency dependence in scotopic flicker sensitivity," Vis. Res. **25**, 115–127 (1985).
28. R. Gortlemeyer and H. Wieman, "Retest reliability and construct validity of critical flicker fusion frequency," Pharmacopsychiatry **15**, 24–28 (1982).
29. R. A. Bone and J. T. Landrum, "Heterochromatic flicker photometry," Arch. Biochem. Biophys. **430**, 137–142 (2004).
30. J. S. Werner, S. K. Donnelly, and R. Kliegl, "Aging and human macular pigment density," Vis. Res. **27**, 257–268 (1987).
31. J. L. Barbur, E. Konstantakopoulou, M. Rodriguez-Carmona, J. A. Harlow, A. G. Robson, and J. D. Moreland, "The macular assessment profile test—a new VDU-based technique for measuring the spatial distribution of the macular pigment, lens density and rapid flicker sensitivity," Ophthalmic Physiol. Opt. **30**, 470–483 (2010).
32. G. Wald and P. K. Brown, "Human rhodopsin," Science **127**, 222–249 (1958).
33. W. Rushton, "Visual pigments in man," in *Handbook of Sensory Physiology. Photochemistry of Vision*, H. J. A. Dartnall, ed. (Springer, 1972), pp. 481–528.
34. H. J. A. Dartnall, "The interpretation of spectral sensitivity curves," Brit. Med. Bull. **9**, 24–30 (1953).
35. M. Alpern, A. B. Fulton, and B. N. Baker, "Self-screening of rhodopsin in rod outer segments," Vis. Res. **27**, 1459–1470 (1987).
36. D. A. Baylor, B. J. Nunn, and J. L. Schnapf, "The photocurrent, noise and spectral sensitivity of rods of the monkey macaca fascicularis," J. Physiol. **357**, 575–607 (1984).
37. E. J. Warrant and D. Nilsson, "Absorption of white light in photoreceptors," Vis. Res. **38**, 195–207 (1998).
38. A. T. Liem, J. E. Keunen, D. van Norren, and J. van de Kraats, "Rod densitometry in the aging human eye," Invest. Ophthalmol. Vis. Sci. **32**, 2676–2682 (1991).
39. G. R. Jackson, C. Owsley, and G. McGwin, Jr., "Aging and dark adaptation," Vis. Res. **39**, 3975–3982 (1999).

40. T. F. Chen, G. V. G. Baranoski, and K. F. Lin, "Bulk scattering approximations for He–Ne laser transmitted through paper," Opt. Express **16**, 21762–21771 (2008).
41. D. M. Gakamsky, B. Dhillon, J. Babraj, M. Shelton, and S. D. Smith, "Exploring the possibility of early cataract diagnostics based on tryptophan fluorescence," J. R. Soc. Interface **8**, 1616–1621 (2011).
42. W. Ambach, M. Blumthaler, T. Schöpf, E. Ambach, F. Katzgraber, F. Daxecker, and A. Daxer, "Spectral transmission of the optical media of the human eye with respect to keratitis and cataract formation," Doc. Ophthalmol. **88**, 165–173 (1994).
43. E. A. Boettner and J. R. Wolter, "Transmission of the ocular media," Invest. Ophthalmol. Vis. Sci. **1**, 776–783 (1962).
44. L. Kolozsv, A. Ngrdi, B. Hopp, and Z. Bor, "UV absorbance of the human cornea in the 240- to 400 nm range," Invest. Ophthalmol. Vis. Sci. **43**, 2165–2168 (2002).
45. R. C. Smith and K. S. Baker, "Optical properties of the clearest natural waters (200–800 nm)," Appl. Opt. **20**, 177–184 (1981).
46. T. J. T. P. van den Berg and H. Spekreijse, "Near infrared light absorption in the human eye media," Vis. Res. **37**, 249–253 (1997).
47. E. R. Gaillard, L. Zheng, J. C. Merriam, and J. Dillon, "Age-related changes in the absorption characteristics of the primate lens," Invest. Ophthalmol. Vis. Sci. **41**, 1454–1459 (2000).
48. H. Bloemendal, W. de Jong, R. Jaenicke, N. H. Lubsen, C. Slingsby, and A. Tardieu, "Ageing and vision: structure, stability and function of lens crystallins," Progr. Biophys. Mol. Biol. **86**, 407–485 (2004).
49. D. van Norren and J. van de Kraats, "Spectral transmission of intraocular lenses expressed as a virtual age," Br. J. Ophthalmol. **91**, 1374–1375 (2007).
50. C. W. Tyler, "Two processes control variations in flicker sensitivity over the life span," J. Opt. Soc. Am. A **6**, 481–490 (1989).
51. C. B. Y. Kim and M. J. Mayer, "Foveal flicker sensitivity in healthy aging eyes. II. Cross-sectional aging trends from 18 through 77 years of age," J. Opt. Soc. Am. A **11**, 1958–1969 (1994).
52. R. A. Weale, "Age and the transmittance of the human crystalline lens," J. Physiol. **395**, 577–587 (1988).
53. B. R. Hammond, J. E. Nanez, C. Fair, and D. M. Snodderly, "Iris color and age-related changes in lens optical density," J. Ophthalmic Physiol. Opt. **20**, 381–386 (2000).
54. K. Sagawa and Y. Takahashi, "Spectral luminous efficiency as a function of age," J. Opt. Soc. Am. A **18**, 2659–2667 (2001).
55. M. C. Gimenez, M. J. Kanis, D. G. M. Beersma, B. A. E. van der Pol, D. van Norren, and M. C. M. Gordijn, "In vivo quantification of the retinal reflectance spectral composition in elderly subjects before and after cataract surgery: implications for the non-visual effects of light," J. Biol. Rhythms **25**, 123–131 (2010).
56. A. Stockman, L. T. Sharpe, and C. Fach, "The spectral sensitivity of the human short-wavelength sensitive cones derived from thresholds and color matches," Vis. Res. **39**, 2901–2927 (1999).
57. N. P. Cottaris, "Artifacts in spatiochromatic stimuli due to variations in preretinal absorption and axial chromatic aberration: implications for color physiology," J. Opt. Soc. Am. A **20**, 1694–1713 (2003).
58. W. N. Charman, "Age, lens transmittance, and the possible effects of light on melatonin suppression," Ophthalmic Physiol. Opt. **23**, 181–187 (2003).
59. F. Delori, D. G. Goger, B. R. Hammond, D. M. Snodderly, and S. A. Burns, "Macular pigment density measured by autofluorescence spectrometry: comparison with reflectometry and heterochromatic flicker photometry," J. Opt. Soc. Am. A **18**, 1212–1230 (2001).
60. J. Hammond, B. R. Wooten, and D. M. Snodderly, "Individual variations in the spatial profile of human macular pigment," J. Opt. Soc. Am. A **14**, 1187–1196 (1997).
61. S. F. Chen, Y. Chang, and J. C. Wu, "The spatial distribution of macular pigment in humans," Curr. Eye Res. **23**, 422–434 (2001).
62. T. van den Berg and K. Tan, "Light transmittance of the human cornea from 320 to 700 nm for different ages," Vis. Res. **34**, 1453–1456 (1994).
63. J. A. J. Van Loo and J. M. Enoch, "The scotopic Stiles-Crawford effect," Vis. Res. **15**, 1005–1009 (1975).
64. J. A. Van Best and E. V. Kuppens, "Summary of studies on the blue-green autofluorescence and light transmission of the ocular lens," J. Biomed. Opt. **1**, 243–250 (1996).
65. J. A. Zuclich, R. D. Glickman, and A. R. Menendez, "In situ measurements of lens fluorescence and its interference with visual function," Invest. Ophthalmol. Vis. Sci. **33**, 410–415 (1992).
66. T. J. T. P. van den Berg, L. Franssen, and J. E. Coppens, "Straylight in the human eye: testing objectivity and optical character of the psychophysical measurement," Ophthalmic Physiol. Opt. **29**, 345–350 (2009).
67. R. A. Weale, "Human lenticular fluorescence and transmissivity, and their effects on vision," Exp. Eye Res. **41**, 457–473 (1985).
68. G. F. Cooper and J. G. Robson, "The yellow colour of the lens of man and other primates," J. Physiol. **203**, 411–417 (1969).
69. N. T. Yu, M. Bando, and J. F. Kuck, Jr., "Fluorescence/Raman intensity ratio for monitoring the pathologic state of human lens," Invest. Ophthalmol. Vis. Sci. **26**, 97–101 (1985).
70. R. A. Weale, "A theoretical link between lenticular absorbance and fluorescence," Proc. Biol. Sci. **263**, 1111–1116 (1996).
71. T. J. van den Berg, "Quantal and visual efficiency of fluorescence in the lens of the human eye," Invest. Ophthalmol. Vis. Sci. **34**, 3566–3573 (1993).
72. J. L. Brown, "Flash blindness," Am. J. Ophthalmol. **60**, 505–520 (1965).
73. R. Gray, S. A. Perkins, R. Suryakumar, B. Neuman, and W. A. Maxwell, "Reduced effect of glare disability on driving performance in patients with blue light–filtering intraocular lenses," J. Cataract Refract.Surg. **37**, 38–44 (2011).
74. T. van den Berg, J. Ijspeert, and P. de Waard, "Dependence of intraocular straylight on pigmentation and light transmission through the ocular wall," Vis. Res. **31**, 1361–1367 (1991).
75. W. J. Geeraets, R. C. Williams, G. Chan, W. T. Ham, D. Guerry, and F. H. Schmidt, "The loss of light energy in retina and choroid," Arch. Ophthalmol. **64**, 606–615 (1960).
76. D. Snodderly, P. Brown, F. Delori, and J. Auran, "The macular pigment. I. Absorbance spectra, localization, and discrimination from other yellow pigments in primate retinas," Invest. Ophthalmol. Vis. Sci. **25**, 660–673 (1984).
77. J. Bowmaker, S. Astell, D. Hunt, and J. Mollon, "Photosensitive and photostable pigments in the retinae of old world monkeys," J. Exp. Biol. **156**, 1–19 (1991).
78. R. Hubbard and A. Kropf, "The action of light on rhodopsin," Proc. Natl. Acad. Sci. USA **44**, 130–139 (1958).
79. C. Grimm, C. E. Rem, P. O. Rol, and T. P. Williams, "Blue light's effects on rhodopsin: photoreversal of bleaching in living rat eyes," Invest. Ophthalmol. Vis. Sci. **41**, 3984–3990 (2000).
80. P. Chen, W. Hao, L. Rife, X. P. Wang, D. Shen, J. Chen, T. Ogden, G. B. Van Boemel, L. Wu, M. Yang, and H. K. Fong, "A photic visual cycle of rhodopsin regeneration is dependent on Rgr," Nat. Genet. **28**, 256–260 (2001).
81. A. Wenzel, V. Oberhauser, E. N. Pugh, T. D. Lamb, C. Grimm, M. Samardzija, E. Fahl, M. W. Seeliger, C. E. Rem, and J. von Lintig, "The retinal G protein-coupled receptor (RGR) enhances isomerohydrolase activity independent of light," J. Biol. Chem. **280**, 29874–29884 (2005).
82. J. Xu, J. Pokorny, and V. C. Smith, "Optical density of the human lens," J. Opt. Soc. Am. A **14**, 953–960 (1997).
83. M. Ozolinsh and P. Paulins, "LED based dual wavelength heterochromatic flicker method for separate evaluation of lutein and zeaxanthin in retina," presented at the International Symposium on Biomedical Engineering and Medical Physics, 10–12 October 2012, Riga, Latvia.
84. M. Potash and B. Jones, "Aging and decision criteria for the detection of tones in noise," J. Gerontol. **14**, 953–960 (1997).
85. D. M. Berson, F. A. Dunn, and M. Takao, "Phototransduction by retinal ganglion cells that set the circadian clock," Science **295**, 1070–1073 (2002).
86. O. Dkhissi-Benyahya, C. Gronfier, W. D. Vanssay, F. Flamant, and H. M. Cooper, "Modeling the role of mid-wavelength cones in circadian responses to light," Neuron **53**, 677–687 (2007).
87. L. S. Mure, P. Cornut, C. Rieux, E. Drouyer, P. Denis, C. Gronfier, and H. M. Cooper, "Melanopsin bistability: a fly's eye technology in the human retina," PLoS ONE **4**, e5991 (2009).